

General Disclaimer

One or more of the Following Statements may affect this Document

- This document has been reproduced from the best copy furnished by the organizational source. It is being released in the interest of making available as much information as possible.
- This document may contain data, which exceeds the sheet parameters. It was furnished in this condition by the organizational source and is the best copy available.
- This document may contain tone-on-tone or color graphs, charts and/or pictures, which have been reproduced in black and white.
- This document is paginated as submitted by the original source.
- Portions of this document are not fully legible due to the historical nature of some of the material. However, it is the best reproduction available from the original submission.

LSS-10

N69-27440

SIMULTANEOUS OPTICAL AND RADIO OBSERVATIONS OF NP 0532*

DNF

Simultaneous optical and radio observations of the Crab Nebula pulsar, NP 0532, were obtained at Lick Observatory and Stanford University respectively, on March 13 and 15. While exact mechanisms responsible for the radio and optical emissions are still not clear, the detection of a time interval (if any) between the optical and radio pulses would be an important test of the various emission theories^{1,2}. Our data show, after correction for interstellar dispersion, that the optical and radio pulses are emitted simultaneously with a phase uncertainty of ± 6 milliseconds which results almost entirely from the uncertainty in the value of the interstellar dispersion. The measured phase delay before correction is accurate to approximately 250 microseconds.

A block diagram of the experiment is shown in Figure 1. Pulses from an ITT FW 130 photomultiplier operated at the prime focus of the 120-inch telescope were counted in a Hewlett-Packard Type 5401A multi-channel analyzer. Each scan through the 1024-channel memory was initiated by an external trigger signal set at the pulsar repetition rate. The rate of scan was variable, and was set as fast as 10 μ s per channel. The trigger signal was provided by a frequency synthesizer and scaler; it was possible to match the apparent period of the pulsar to better than 1 part in 10^7 , allowing long integration times without degrading the pulse shape. The trigger signal was transmitted over a VHF radio link to the 150-foot parabola at Stanford, 48 km to the west. A second synthesizer at Stanford was adjusted to the same frequency and phase as the first. Its scaled output was used to trigger a Hewlett-Packard Type 5480A analog signal averager, which analyzed 424 MHz radio pulses, operating in much the same way as the multichannel

* Contributions from the Lick Observatory, No. 297.

Pages - 9
code # 1

CRB1227

AT 30

analyzer at Lick. We estimate that the two trigger signals were synchronized to $\pm 50 \mu\text{s}$ over any 1-hour period after compensation for travel time and other systematic effects.

Figure 2 shows the results of one observation on March 15. The optical pulses were measured in white light with a 5.5 arcsec diaphragm. The analyzer had a channel width of $50 \mu\text{s}$; the trace is the sum of 2000 scans. Smearing of the pulses due to a slight drift of the trigger signal is about $60 \mu\text{s}$, so that the pulse shapes shown are essentially unaffected by the equipment. The half-power widths of the main pulse and subpulse are 1.5 and 2.6 ms; the ratio of their peak amplitudes is 3.5.

The radio pulses were observed at 424.00 MHz in a 600 kHz bandwidth. The tracing in Figure 2 is an average of about 22,000 pulses, indicating the weakness of the radio signal; the signal-to-noise ratio is low partly because the Crab Nebula is itself a very strong continuous radio source. Dispersion across the receiver bandwidth and a 1 ms time constant on the receiver output have broadened the pulses by about 5 ms, so that little information on the intrinsic widths is available; the observed widths do not disagree with the optical widths. The ratio of main pulse to subpulse peak amplitude, however, is about 1.2 instead of the optical value of 3.5. Observations at Arecibo³ give about the same ratio for the radio pulses; the disagreement with the optical value may be due to polarization effects, as both the Arecibo and Stanford antennas are circularly polarized.

The positions of the optical and radio pulses in Figure 2 do not represent the time relationship at the source because the radio pulses have been delayed considerably by the interstellar medium. A pulse observed at frequency ν will have been delayed by Δt seconds, where

$$\Delta t = \frac{1}{v^2} \left(-\frac{\int n_e dl}{7.4378 \times 10^{14}} \right)$$

Here v is in MHz, and the integrated electron density is in electrons/cm². For NP 0532, the integrated density is $(1.755 \pm 0.007) \times 10^{20}$ el/cm² (ref. 3); a pulse at 424.00 MHz is delayed 1312.49 ms, or more than 39 periods. The optical pulse is delayed about 2×10^{-13} sec. Because the optical and radio pulses may not come from the same regions there is a possible ambiguity of an integral number of periods in determining the delay between the optical and radio pulses. In what follows we will take this number to be zero, thus making the assumption that the various emission centers are less than 10,000 km apart.

Three successful simultaneous observations of optical and radio pulses were made, each lasting about 30 minutes. The results are summarized in Table 1. The line headed Observed Radio Delay gives the apparent time between the peak of the main optical pulse and the peak of the main radio pulse; corrections for small phase differences in the trigger signals, travel times of the trigger and pulsar signals over the 48 km baseline, and propagation delays in the receiving systems have been made. The probable errors quoted for the observed delay are due almost entirely to errors in measuring the position of the weak radio pulse; the error quoted for March 13 is larger due to a lower signal-to-noise ratio at that time. The error in the calculated delay is due to uncertainty in the integrated electron density.

A weighted average of the data indicates that the radio pulse arrives sooner than expected by 0.63 ms, with an experimental error of ± 0.25 ms and a systematic error of ± 6.0 ms due to the uncertain electron density.

The difference in arrival times is obviously not significant in view of the total error involved; at present we can only conclude that the radio and optical pulses are emitted within 6 ms of each other. However, when more accurate values for the integrated electron density become available, the observed delay values are sufficiently precise to determine time intervals at the source as small as 0.25 ms. Time delays of this magnitude are important for radio emission mechanisms of the type proposed by Gold², in which the observed pulses are produced at a transverse distance from a neutron star where the peripheral speed is near the speed of light. For NP 0532, this transverse distance is 1600 km. The observed time delay of less than 6 ms requires a transverse distance between optical and radio emission centers of less than 1800 km; if the delay proves to be less than 0.25 ms, the distance would be less than 75 km.

Alternatively, we can assume that the optical and radio pulses are emitted simultaneously. We then can derive an accurate value for the integrated electron density from the observed pulse arrival times. The delays in Table 1 give a value of $(1.7542 \pm .0003) \times 10^{20}$ el/cm².

We are grateful to the Hewlett-Packard company for providing some of the equipment used in the experiment. This work was supported at Stanford University by the Air Force Office of Scientific Research and the National Aeronautics and Space Administration. The observations at Lick Observatory have been supported, in part, by the National Science Foundation and by the National Aeronautics and Space Administration.

E. K. Conklin
H. T. Howard

Stanford University
Stanford, California 94305

J. S. Miller
E. J. Wampler

Lick Observatory
University of California
Santa Cruz, California 95060

Received _____

¹Chiu, H.-Y., Canuto, V., and Fassio-Canuto, L., Nature, 221, 529 (1969).

²Gold, T., Nature, 221, 25 (1969).

³Comella, J. M., Craft, H. D., Lovelace, R. V. E., Sutton, J. M., and Tyler, G. L., Nature, 221, 453 (1969).

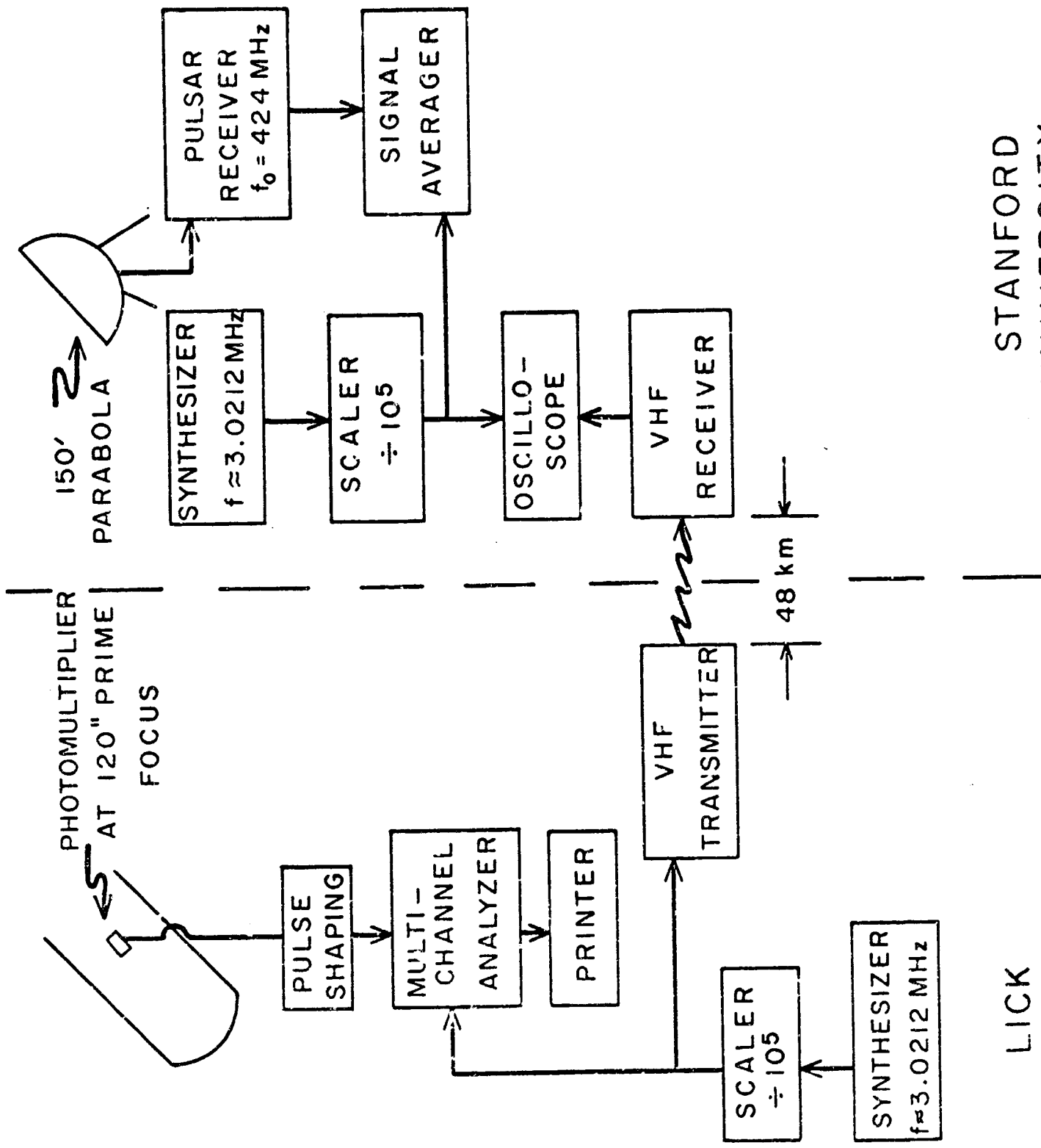
FIGURE CAPTIONS

Figure 1. Block diagram of the simultaneous experiment.

Figure 2. Simultaneous observations on March 15, 2000-2030 PST. (a) 5 minute average of white light optical pulses; (b) 25 minute average of 424 MHz radio pulses. The abscissa is the time after a trigger signal at each site. The dispersion delay and bandwidth broadening of the radio pulses have not been removed. S = subpulse; M = main pulse.

TABLE I - SUMMARY OF OBSERVATIONS

Date	Mar 13	Mar 15	Mar 15
Time (PST)	2000-2020	2000-2030	2100-2130
Apparent Period (ms)	33.09876	33.09885	33.09887
Radio Frequency (MHz)	423.28	424.00	424.00
Observed Radio Delay (ms)	26.13 \pm 0.60	21.09 \pm 0.40	20.48 \pm 0.40
Calculated Delay (ms)	1316.96 \pm 6.0	1312.49 \pm 6.0	1312.49 \pm 6.0
Calculated Delay minus 39 Periods (ms)	26.11 \pm 6.0	21.63 \pm 6.0	21.63 \pm 6.0
Difference (ms)	+0.02 \pm 6.0	-0.54 \pm 6.0	-1.15 \pm 6.0



STANFORD
UNIVERSITY

LICK
OBSERVATORY

